

Fluorine-vacancy complexes in Si-SiGe-Si structures

D. A. Abdulmalik and P. G. Coleman^{a)}

Department of Physics, University of Bath, Bath BA2 7AY, United Kingdom

H. A. W. El Mubarek and P. Ashburn

School of Electronics and Computer Science, University of Southampton,
Southampton SO17 1BJ, United Kingdom

(Received 23 April 2007; accepted 29 May 2007; published online 13 July 2007)

Fluorine-vacancy (FV) complexes have been directly observed in the $\text{Si}_{0.94}\text{Ge}_{0.06}$ layer in a Si-SiGe-Si structure, using variable-energy positron annihilation spectroscopy (VEPAS). These complexes are linked to the significant reduction of boron diffusion in the SiGe layer via interstitial trapping. Vacancies were introduced into the samples by ion implantation with 185 keV F^+ at doses in the range 9×10^{14} to $1 \times 10^{16} \text{ cm}^{-2}$; the samples were subsequently subjected to rapid annealing in nitrogen ambient at 950 °C for 30 s. The VEPAS results, in combination with F profiles obtained by secondary ion mass spectrometry, are consistent with F_{4n}V_n complexes being associated with the SiGe layer and that they preferentially accumulate at the Si/SiGe interfaces. Their concentration is critically dependent on annealing temperature, decreasing significantly after annealing at 1000 °C.

© 2007 American Institute of Physics. [DOI: [10.1063/1.2753573](https://doi.org/10.1063/1.2753573)]

I. INTRODUCTION

Fluorine as an implant in Si has been the subject of extensive studies recently,^{1–4} because of its effectiveness in retarding the transient-enhanced diffusion (TED) of boron, the key to achieving ultra-shallow junctions and consequently miniature Si-based devices. The formation of fluorine-vacancy (FV) complexes has been proposed as a likely candidate for the physical mechanism through which boron TED is reduced, acting as traps for the Si interstitials, which enhance the diffusion. Recent FV studies have included experimental positron annihilation spectroscopy (PAS)^{5–7} and secondary ion mass spectrometry (SIMS) of solid phase, epitaxially regrown Si⁸ as well as *ab initio* calculations.^{9,10} Models of $\sim 2\text{--}3$ F atoms in FV clusters^{5,8} or F_{3n}V_n with n most probably 1 and/or 2 (Ref. 7) were found to be plausible assumptions in explaining experimental results, while various F_nV_m (for $n=2m+2$, with up to four vacancies and an F:V ratio between 4 and 2) energetically favorable configurations were proposed theoretically.^{9,10}

In contrast, there is little knowledge to date on the behavior of F in SiGe. SiGe is a promising material in micro-electronic technology, especially in the fabrication of heterojunction bipolar transistors (HBTs). While some studies have been performed using PAS to investigate vacancy-type defects and their complexes in SiGe layers,¹¹ none have focused on F in SiGe structures. In this work we report results on the use of variable-energy PAS (VEPAS) to investigate the behavior of F in a layered structure of Si-SiGe-Si analogous to that used in HBTs.

II. EXPERIMENTAL PROCEDURE

Low pressure chemical vapor deposition at 850 °C (growth A) and 800 °C (growth B) was used to grow boron

marker layers for monitoring boron diffusion. The growth temperatures were chosen as being typical of those used in device epitaxy. The growth A samples comprised a 400 nm undoped silicon layer, a 50 nm $\text{Si}_{0.94}\text{Ge}_{0.06}$ layer with a peak boron concentration of $5 \times 10^{18} \text{ cm}^{-3}$, and a 130 nm undoped silicon cap layer; the substrate was a very-low-doped $\langle 100 \rangle$ Si wafer. The growth B samples comprised a 400 nm *n*-type silicon layer ($10^{18} \text{ P cm}^{-3}$), a 40 nm $\text{Si}_{0.94}\text{Ge}_{0.11}$ layer with a peak boron concentration of $1.2 \times 10^{19} \text{ cm}^{-3}$, and a 130 nm *n*-type silicon cap layer ($10^{18} \text{ P cm}^{-3}$). Thus the type A samples form an *i-p-i* structure, whereas the type B samples form an *n-p-n* structure. Some of the type A and type B samples were then implanted with P^+ ions at 288 keV and $6 \times 10^{13} \text{ cm}^{-2}$. Type A samples were implanted with 185 keV F^+ ions at a dose of either 9×10^{14} or $1.85 \times 10^{15} \text{ cm}^{-2}$ and type B samples were implanted with 185 keV F^+ ions at a dose of either 2.3×10^{15} or $1 \times 10^{16} \text{ cm}^{-2}$. All samples were then subjected to rapid thermal annealing in a nitrogen ambient at 950 °C for 30 s. As-implanted and as-grown samples were also produced as controls.

In VEPAS, positrons in the energy range 0.5–24 keV were implanted into the samples to enable depth profiling from the surface to $\sim 2.5 \mu\text{m}$. As positrons enter the material they rapidly thermalize, then diffuse until they either annihilate freely with electrons or are trapped by vacancy-type defects and eventually annihilate via two γ rays in approximately opposite directions and 511 keV energy. Doppler broadening of the 511 keV annihilation line, resulting from the momentum of the annihilated electrons, is measured with a high-purity Ge detector and characterized by the simple line-shape *S* parameter, defined as the fraction of counts in a central region of the annihilation line.

The concentration depth profiles of ^{74}Ge and ^{19}F were measured using secondary ion mass spectroscopy (SIMS).

^{a)}Electronic mail: p.g.coleman@bath.ac.uk

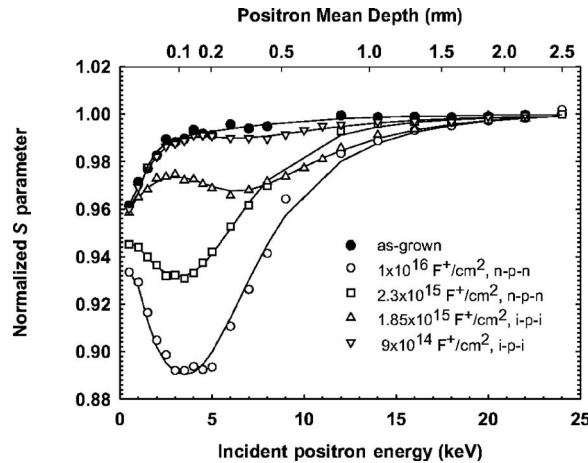


FIG. 1. S parameter versus incident positron energy for samples implanted with 185 keV F^+ at 1×10^{16} , 2.3×10^{15} , 1.85×10^{15} , and 9×10^{14} cm^{-2} , and annealed at 950°C for 30 s. The data for an as-grown sample are also shown. The solid lines are fits obtained using VEPFIT.

III. RESULTS

Figure 1 presents the variation of the S parameter, normalized to a value of unity for the bulk material, with the incident positron energy E for the four samples implanted with 185 keV F^+ ions at 1×10^{16} ($n-p-n$), 2.3×10^{15} ($n-p-n$), 1.85×10^{15} ($i-p-i$), and 9×10^{14} cm^{-2} ($i-p-i$) after annealing at 950°C for 30 s. None of the samples had P^+ implants. The behavior of the as-grown sample (type B) is also shown as a reference. The mean depth (z) probed by the positrons with energy E (keV) is also shown in the figure, where $z \approx 17.2 E^{1.6}$ nm. $S(E)$ for the as-implanted samples (see, e.g., Figs. 2 and 3) show no enhanced vacancy response in the SiGe layer. After annealing, S parameters below the bulk value, S_B , were measured in all samples for a mean depth up to $\sim 0.9 \mu\text{m}$, being most marked between ~ 0.06 – $0.2 \mu\text{m}$ in the samples implanted with the two highest F doses and deeper (between ~ 0.2 – $0.6 \mu\text{m}$) in the two lowest-dose samples (9×10^{14} and 1.85×10^{15} cm^{-2}). The survival of vacancies after annealing, and the observation of S values below unity, is attributed to the accumulation of F_xV_y complexes in specific regions. This behavior was observed earlier by Pi *et al.*⁶ and was attributed to the presence of F in the vicinity of the vacancies; it is well known that annihilation with F electrons leads to a reduction in the vacancy S parameter.¹² El Mubarek *et al.* linked F_xV_y complexes with the mechanism underlying B thermal diffusion reduction in similar samples.¹³

The difference in the position of the dip in $S(E)$ —3.5 and 6 keV for the samples implanted with the highest and lowest two F doses, respectively—can be understood in terms of the presence of electric fields in the highest-dose samples (both $n-p-n$ structures) and the relatively negligible fields in the two lowest-dose samples ($i-p-i$). In the former case the field drifts the diffusing positrons to the SiGe layer from both sides, thereby enhancing the sensitivity of VEPAS to the FV complexes formed there. In the latter case a greater fraction of the implanted positrons sense the damage beneath the SiGe layer and, therefore, a broader response is observed centered at around 6 keV, corresponding to depths close to the peak of damage caused by 185 keV F^+ ($\sim 0.3 \mu\text{m}$, as calculated by TRIM¹⁴). In a study of similar samples using SIMS and transmission electron microscopy (TEM), El Mubarek *et al.* observed deep F peaks in the same range in SIMS profiles and concluded that these were due to F trapping at dislocation loops together with defects at the growth interface.¹³ Therefore, in summary, the dip in $S(E)$ at ~ 3.5 keV corresponds to F_xV_y complexes in the SiGe layer, and the broader dip at ~ 6 keV to F_xV_y complexes principally in the Si beneath the SiGe layer.

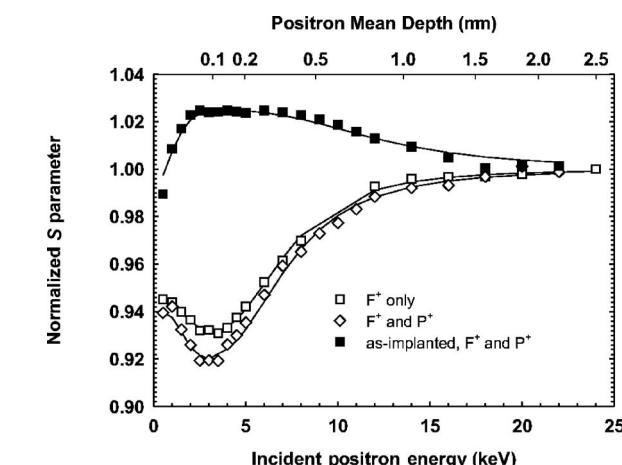


FIG. 2. Comparison between the behavior of the $n-p-n$ sample implanted with 2.3×10^{15} F^+ cm^{-2} with and without P^+ implants. Data for the as-implanted sample (with F and P) are also shown as a reference.

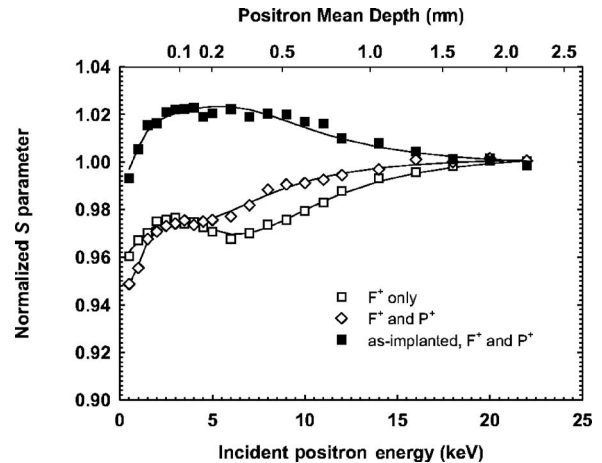


FIG. 3. Comparison between the behavior of the $i-p-i$ sample implanted with 1.85×10^{15} F^+ cm^{-2} with and without P^+ implants. Data for the as-implanted sample (with F and P) are also shown as a reference.

plexes in specific regions. This behavior was observed earlier by Pi *et al.*⁶ and was attributed to the presence of F in the vicinity of the vacancies; it is well known that annihilation with F electrons leads to a reduction in the vacancy S parameter.¹² El Mubarek *et al.* linked F_xV_y complexes with the mechanism underlying B thermal diffusion reduction in similar samples.¹³

The difference in the position of the dip in $S(E)$ —3.5 and 6 keV for the samples implanted with the highest and lowest two F doses, respectively—can be understood in terms of the presence of electric fields in the highest-dose samples (both $n-p-n$ structures) and the relatively negligible fields in the two lowest-dose samples ($i-p-i$). In the former case the field drifts the diffusing positrons to the SiGe layer from both sides, thereby enhancing the sensitivity of VEPAS to the FV complexes formed there. In the latter case a greater fraction of the implanted positrons sense the damage beneath the SiGe layer and, therefore, a broader response is observed centered at around 6 keV, corresponding to depths close to the peak of damage caused by 185 keV F^+ ($\sim 0.3 \mu\text{m}$, as calculated by TRIM¹⁴). In a study of similar samples using SIMS and transmission electron microscopy (TEM), El Mubarek *et al.* observed deep F peaks in the same range in SIMS profiles and concluded that these were due to F trapping at dislocation loops together with defects at the growth interface.¹³ Therefore, in summary, the dip in $S(E)$ at ~ 3.5 keV corresponds to F_xV_y complexes in the SiGe layer, and the broader dip at ~ 6 keV to F_xV_y complexes principally in the Si beneath the SiGe layer.

$S(E)$ data for two of the samples are shown in Figs. 2 and 3 with F^+ implants only and with F^+ and P^+ implants. The $n-p-n$ samples in Fig. 2 were implanted with 2.3×10^{15} F^+ cm^{-2} and the $i-p-i$ samples in Fig. 3 with 1.85×10^{15} F^+ cm^{-2} . In Fig. 2 positrons can detect more FV complexes in the SiGe layer when both F^+ and P^+ are implanted, a lower S parameter being measured in the latter case. The extra complexes are formed because P -implantation introduces additional vacancies and, as there is excess F at this dose, F can associate with them. The fitted layer S parameters for the two data sets shown in Fig. 2

suggest an increase in vacancy concentration in the SiGe layer of approximately 20% when P^+ ions are implanted, a figure which matches well the increase in F concentration in the layer according to SIMS.

For the *i-p-i* sample implanted with P^+ and $1.85 \times 10^{15} F^+ \text{ cm}^{-2}$ (Fig. 3), the P-implantation overdopes the intrinsic regions in the *i-p-i* structure, converting it to an *n-p-n* structure. This introduces an electric field acting over a distance of $\sim 10^2 \text{ nm}$, which makes the positrons less sensitive to the defects in the Si layer beneath the SiGe and consequently more sensitive to those in the SiGe layer, where again the slightly lower S value implies that more FV complexes are formed there if P is implanted. Accordingly, it can be inferred that P-implantation increases FV clustering in the SiGe region as well as positron sensitivity to the clusters.

VEPAS data were also recorded for the $1 \times 10^{16} F^+ \text{ cm}^{-2}$ sample with and without P-implantation (not shown here). Exactly the same S parameter was measured, implying saturation positron trapping in the FV defects in both cases, so that the extra vacancies introduced by P^+ implantation resulted in no change in VEPAS response.

IV. DISCUSSION

The $S(E)$ data for the as-grown *n-p-n* sample in Fig. 1 exhibit an increase from its surface value to the bulk with a notably short diffusion length. This is attributed to electric fields drifting positrons toward the SiGe layer, which thus greatly reduce positron diffusion to the surface.

The solid lines behind the data points in the figures are fits obtained using VEPFIT.¹⁵ The samples are modeled as layered structures; electric fields in the near-surface region resulting from band bending and of $+2 \times 10^3$ and $-1 \times 10^3 \text{ V cm}^{-1}$ in the Si layers on each side of the SiGe layer were incorporated in the model to fit the P-doped samples. While the fitting was relatively insensitive to positron diffusion lengths, sensible self-consistent fits were always achieved. As the F dose increases the S parameter associated with the SiGe layer, S_{SiGe} , decreases from 0.995 to 0.878, as more FV clusters reside there; saturation trapping is believed to be reached for the F dose of $1 \times 10^{16} \text{ cm}^{-2}$, so that the S parameter characteristic of the FV complex, S_D , is ~ 0.88 . This is consistent with the authors' and others' earlier measurements in Si.⁷ While the cap Si layer could be fitted with bulk (defect-free) Si parameters, the Si layer beneath the SiGe, extending to $0.6 \mu\text{m}$ could not; a region centered at $\sim R_P$ exhibits fitted S values, which imply a combination of F-related defects, which could include FV complexes in the vacancy-rich zone, F-interstitial (FI) defects in the I-rich zone beyond R_P , and F agglomerates and precipitates around R_P (as seen in Si in Ref. 6). In the *i-p-i* samples, positrons are not drifted to the SiGe layer and are thus more sensitive to the F-related defects in the underlying Si layer; this explains the observation of a lower S parameter in the raw data for $1.85 \times 10^{15} \text{ cm}^{-2}$ F dose than in the data for the higher F dose of $2.35 \times 10^{15} \text{ cm}^{-2}$ at $\sim 10 \text{ keV}$.

In an attempt to achieve an insight into the nature of the FV complexes the vacancy concentration C_v , derived from the VEPAS data, has been compared with the F concentra-

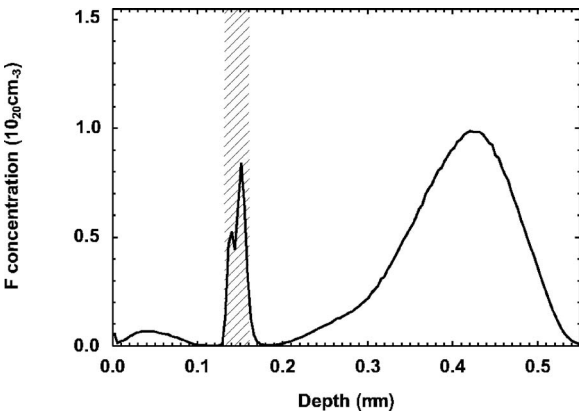


FIG. 4. SIMS profile of F for the sample implanted with 185 keV F^+ at $2.3 \times 10^{15} \text{ cm}^{-2}$ and annealed at $950 \text{ }^\circ\text{C}$ for 30 s. The shaded region indicates the full-width-at-half-maximum of the Ge SIMS profile, corresponding to the SiGe layer.

tion C_F , derived from SIMS data. C_v (in cm^{-3}) in the SiGe layer was calculated from the fitted S parameter in the layer, S_{SiGe} , as

$$C_v = 5 \times 10^{22} [\lambda_B (S_{\text{SiGe}} - 1) / \nu (S_D - S_{\text{SiGe}})], \quad (1)$$

where λ_B is the positron annihilation rate in perfect Si ($= 4.54 \times 10^9 \text{ s}^{-1}$)¹⁶ and ν is the specific trapping rate for positrons ($\approx 3n \times 10^{14} \text{ s}^{-1}$) in clusters of n vacancies.¹⁷

Let us first consider a model in which the positron trapping sites in the SiGe layer are uniformly distributed throughout the layer. The average C_F over the layer, as obtained by SIMS, is between 20 and 50 times higher than C_v . This implies that either (a) some of the F may be forming FV complexes, such as the $F_{3n}V_n$ seen in Si,⁷ and that the rest (perhaps 85%–95%) are left isolated or form F agglomerates or precipitates, or (b) all the F in the SiGe layer form precipitates and the positrons are trapped in vacancylike defects on their surfaces. If all the positron trapping sites formed in the layer were precipitates, then trapping of positrons would become limited by their diffusion to the defect sites, in which case diffusion-limited trapping model would become important.¹⁸ Using this model the concentration of precipitates, N , can be estimated; for example, for our sample that is implanted with $2.3 \times 10^{15} F^+/\text{cm}^2$, $N \approx 10^9 \text{ cm}^{-3}$, implying $\geq 10^{10} \text{ F}$ per precipitate. These precipitates would be a few μm in diameter, which is unreasonably large.

As uniform trapping throughout the SiGe layer seems unlikely, we turn to an alternative model. Interrogation of the F SIMS profiles such as that shown in Fig. 4 reveals that F could be accumulating at the two heterojunction interfaces between the SiGe and the Si layers (Fig. 4). The shallow F peaks were shown to be correlated with the reduction of boron thermal diffusion by El-Mubarek *et al.*¹³ The influence of defects on F profiles after annealing at temperatures above $500 \text{ }^\circ\text{C}$ was observed in an early study of Si implanted with BF_2^+ .¹⁹ In this work, gettering of F was observed in damaged regions and at the interfaces between crystalline and amorphous regions.

In light of these observations, VEPFIT was employed to fit the VEPAS data with the assumption that all of the FV defects associated with the SiGe layer are at the two hetero-

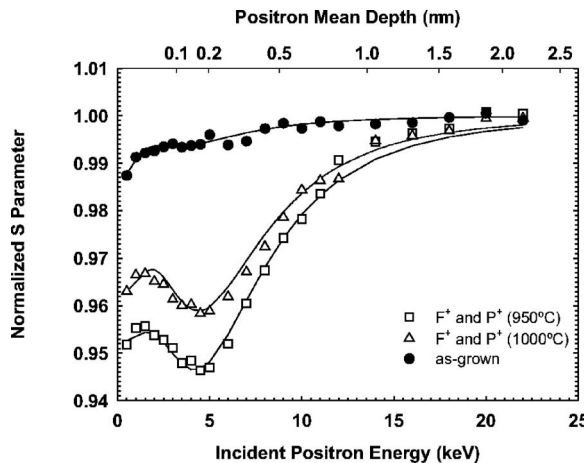


FIG. 5. $S(E)$ curves for Si-SiGe-Si samples implanted with 185 keV F^+ at $2.3 \times 10^{15} \text{ cm}^{-2}$ and 288 keV P^+ at $6 \times 10^{13} \text{ cm}^{-2}$ annealed at 950 °C and 1000 °C for 30 s. Data for an as-grown sample are shown as a reference.

interfaces on each side of the layer, of widths consistent with the SIMS profiles for F. For the sample implanted with $1.85 \times 10^{15} \text{ F cm}^{-2}$, VEPFIT gave interface S parameters corresponding to a total C_v of $7.5 \times 10^{18} \text{ cm}^{-3}$, approximately one quarter of the total C_F in the two interfaces from SIMS. This is consistent with $F_{4n}V_n$ complexes, not far from the $F_{3n}V_n$ complexes (with n most probably 1 and/or 2) proposed by the authors⁷ and other researchers^{5,8} in Si structures.

VEPAS and SIMS data for the region above the SiGe layer, and in F-implanted epitaxial Si control samples, suggest preferential migration of F toward the surface. This has been observed by Pi *et al.*⁶ and also earlier by Jeng *et al.*²⁰ in samples implanted with 30 keV F^+ at doses of 10^{12} and 10^{13} cm^{-2} and annealed for 30 min at temperatures between 300 °C and 1050 °C. Jeng *et al.*²⁰ noticed anomalous rapid diffusion of F at temperatures higher than 550 °C, and they suggested that this behavior could be associated with temperature-dependent F complex formation.

Finally, two samples with SiGe layers (not identical to those used above) were implanted with 185 keV F^+ at $2.3 \times 10^{15} \text{ cm}^{-2}$ and 288 keV P^+ at $6 \times 10^{13} \text{ cm}^{-2}$, then rapid thermal annealed for 30 s at (a) 950 °C and (b) 1000 °C. $S(E)$ is shown in Fig. 5 for these samples as well as, for reference, an as-grown sample. FV complex formation is again evidenced by the low S up to $\sim 0.7 \mu\text{m}$. The increase in S after the higher-temperature anneal suggests a reduction in the concentration and/or size of the FV complexes; if one assumes only the former, then this corresponds to a 40% reduction in defect concentration.

V. CONCLUSION

This work has confirmed that VEPAS can be used directly to observe the formation of FV complexes in SiGe

structures where F implantation has been shown to eliminate boron TED and reduce boron thermal diffusion—here, in Si-SiGe-Si structures implanted with F ions (at an energy chosen so that the SiGe layer lies within the vacancy-rich region of the fluorine damage profile) and rapidly thermal annealed. The present results, together with SIMS evidence, are consistent with the accumulation of $F_{4n}V_n$ complexes at the heterojunction interfaces. The VEPAS response to the FV complexes decreases if the annealing temperature is increased from 950 °C to 1000 °C, suggesting that the efficacy of this method for boron diffusion reduction depends critically on annealing temperature.

ACKNOWLEDGMENTS

DAA is grateful to the State of Qatar for a government scholarship. Dr. Huda El Mubarek is a Royal Academy of Engineering and EPSRC Research Fellow and wishes to thank the Royal Academy of Engineering and EPSRC for funding her research. The authors are grateful for the support of the EU FP6 Co-ordination Project CADRES.

- ¹G. M. Lopez, V. Fiorentini, G. Impellizzeri, S. Mirabella, and E. Napolitani, Phys. Rev. B **72**, 045219 (2005).
- ²M. N. Kham, H. A. W. El Mubarek, J. M. Bonar, and P. Ashburn, Mater. Sci. Eng., B **124-125**, 192 (2005).
- ³T. Noda, J. Appl. Phys. **96**, 3721 (2004).
- ⁴G. Impellizzeri, J. H. R. dos Santos, S. Mirabella, E. Napolitani, A. Carnera, and F. Priolo, Nucl. Instrum. Methods Phys. Res. B **230**, 220 (2005).
- ⁵P. J. Simpson, Z. Jenei, P. Asoka-Kumar, R. R. Robison, and M. E. Law, Appl. Phys. Lett. **85**, 1538 (2004).
- ⁶X. D. Pi, C. P. Burrows, and P. G. Coleman, Phys. Rev. Lett. **90**, 155901 (2003).
- ⁷D. A. Abdulmalik, P. G. Coleman, N. E. B. Cowern, A. J. Smith, B. J. Sealy, W. Lerch, S. Paul, and F. Cristiano, Appl. Phys. Lett. **89**, 052114 (2006).
- ⁸N. E. B. Cowern, B. Colombeau, J. Benson, A. J. Smith, W. Lerch, S. Paul, T. Graf, F. Cristiano, X. Hebras, and D. Bolze, Appl. Phys. Lett. **86**, 101905 (2005).
- ⁹M. Diebel and S. T. Dunham, Phys. Rev. Lett. **93**, 245901 (2004).
- ¹⁰G. M. Lopez and V. Fiorentini, Appl. Phys. Lett. **89**, 092113 (2006).
- ¹¹J. Slotte, Nucl. Instrum. Methods Phys. Res. B **253**, 130 (2006).
- ¹²A. Uedono, T. Kitano, K. Hamada, T. Moriya, T. Kawano, S. Tanigawa, R. Suzuki, T. Ohdaira, and T. Mikado, Jpn. J. Appl. Phys., Part 1 **36**, 2571 (1997).
- ¹³H. A. W. El-Mubarek, M. Karunaratne, J. M. Bonar, G. D. Dilliway, Y. Wang, P. L. F. Hemment, A. F. Willoughby, and P. Ashburn, IEEE Trans. Electron Devices **52**, 518 (2005).
- ¹⁴J. F. Ziegler, J. P. Biersack, and U. Littmark, *The Stopping and Range of Ions in Solids* (Pergamon, New York, 1985).
- ¹⁵A. van Veen, H. Schut, J. De Vries, R. A. Hakvoort, and M. R. Ijppma, AIP Conf. Proc. **218**, 171 (1990).
- ¹⁶S. Dannefaer, J. Phys. C **15**, 599 (1982).
- ¹⁷P. J. Schultz, E. Tandberg, K. G. Lynn, B. Nielson, T. E. Jackman, M. W. Denhoff, and G. C. Aers, Phys. Rev. Lett. **61**, 187 (1988).
- ¹⁸P. G. Coleman, N. B. Chilton, and J. A. Baker, J. Phys.: Condens. Matter **2**, 9355 (1990).
- ¹⁹M. Y. Tsai, D. S. Day, B. G. Streetman, P. Williams, and C. A. Evans, Jr., J. Appl. Phys. **50**, 188 (1979).
- ²⁰S.-P. Jeng, T.-P. Ma, R. Canteri, M. Anderleb, and G. W. Rubloff, Appl. Phys. Lett. **61**, 1310 (1992).